Journal of Intelligent Manufacturing
https://doi.org/10.1007/s10845-023-02288-w

A rotary extrusion system with a rectangular-orifice nozzle: toward adaptive resolution in material extrusion additive manufacturing

Bahar Gharehpapagh[1] · Ugur M. Dilberoglu[1] · Ulas Yaman[1] · Melik Dolen[1]

Received: 17 February 2023 / Accepted: 24 November 2023
© The Author(s) 2024

Abstract
Material extrusion additive manufacturing (MEAM) has revolutionized the production of complex designs while minimizing the amount of effort required due to its simple production pipeline. However, MEAM naturally comes with a well-known trade-off; higher build resolution often tends to enhance the product quality at the cost of a slower build rate. Nozzles, the standard tool for thermoplastic extrusion in MEAM, have evolved into a crucial component of the process for controlling the product's build resolution. The purpose of this study is to investigate the details of a novel extrusion system that makes use of a rotating nozzle with an unconventional aperture, in contrast to its typical (i.e., circular-orifice) counterparts. The unique nozzle configuration that lacks axial symmetry allows for precise control over the effective dimension of the extrusion via rotational guiding. By positioning the oblong orifice at intermediate orientations, the presented approach seeks to provide continuously variable intralayer and interlayer resolutions for MEAM processes. This paper explores the distinctive characteristics of this new nozzle design as well as the potential uses of the novel extrusion system. The outcomes of the conducted tests demonstrate the proof-of-concept for creating variable bead width within the layers, in addition to adaptable layer heights throughout the 3D objects. Possible limitations of the new approach and future perspectives are discussed in detail.

Keywords Material extrusion · Adaptive resolution · Rectangular-orifice nozzle · Variable bead width

Introduction

Additive Manufacturing (AM) has the potential to catch up with conventional manufacturing methods in the upcoming decades. Today, the method offers a multitude of advantages: (i) simplicity in the processing pipeline; (ii) competitiveness in prototyping; (iii) design flexibility; (iv) production of objects with extremely complex geometries. Nevertheless, it has not yet resulted in the well-anticipated effects in industrial applications due to the quality issues that have not been addressed so far (Dilberoglu et al., 2017).

Material extrusion, which is based on the molten thermoplastic buildup, has become a widespread method among the standard AM technologies. In the most common Material Extrusion Additive Manufacturing (MEAM) based process, the base material in filament form is selectively dispensed through a hot nozzle and deposited on a planned tool path (Additive manufacturing—General principles—Terminology, 2015). The integral volume of the solidified material represents the 3D object manufactured. This technology is often referred to as Fused Filament Fabrication (FFF) or Fused Deposition Modeling (FDM).

Since the products of MEAM are simply the combined volume of continuous tubular thermoplastic beads, the strategies for the extrusion and selective placement of those beads form the essence of the process planning for this technology. Here, the ***bead*** refers to the semi-liquid strands coming out of the heated nozzle that has continuously been cooled while being deposited on the traced trajectory (Tan et al., 2020). In typical MEAM processes, ***nozzles*** have evolved into the stan-

✉ Bahar Gharehpapagh
bahar.gharehpapagh@metu.edu.tr

Ugur M. Dilberoglu
ugur.dilberoglu@metu.edu.tr

Ulas Yaman
uyaman@metu.edu.tr

Melik Dolen
dolen@metu.edu.tr

[1] Mechanical Engineering Department, Middle East Technical University, 06800 Ankara, Turkey

Published online: 08 January 2024

dard tool for extrusion. Filamentous thermoplastic material, fed from the inlet opening, is ejected in the form of cylindrical beads. During extrusion, the diameter of the nozzle's orifice controls the size of the formed beads. Consequently, nozzle selection has the greatest influence on ***build resolution***. For instance, a nozzle with a small opening is preferred for better surface quality at the expense of a longer fabrication time.

Despite the trade-off between the part's quality and the fabrication speed, the active nozzle is not changed in a routine FFF process. In common practice, a specific nozzle is allocated in the process plan and deposits the beads in a predetermined size. Either the build resolution or the build rate will be a bottleneck with the current approach. In the last decade, however, researchers have proposed in-process tuning of the width of the extruded lines, or simply the ***bead width*** (BW), to overcome this bottleneck. Analysis of the existing literature revealed that two fundamental principles can be applied to adjust the BW: (i) control of material flow and (ii) control of the extrusion opening.

Extrusion in traditional production has been used to manufacture objects with a fixed cross-sectional profile in the size (and shape) of the die outlet opening. Due to the favorable flow characteristics of the thermoplastics, on the other hand, the size of the extruded profile can be manipulated to some extent in FFF. Recently, researchers have been able to control the bead size with the nozzle's modulated flow rate and traversal speed. Nevertheless, the methods aiming to control the flow have been applicable in a limited range, i.e., constrained by the basic dimensions of the nozzle's outlet opening. In ideal conditions, the extrusion flow rate should synergize with the movement along the extrusion path. Otherwise, over-extrusion or under-extrusion problems are likely to be observed. Lately, researchers have been seeking the best synchronous extrusion settings for ***variable bead width*** (VBW) in FFF.

In a recent study, Wang et al. (2019) reported the relationship between the extrusion flow rate and the BW for various layer thicknesses. Kuipers et al. (2020) have introduced a framework to generate a toolpath with adaptive width. By taking into account the back pressure correction in their Bowden-tube hardware system, they are able to extrude beads at varying levels as a function of the extrusion rate of the filament and the linear movement speed (Kuipers et al., 2020). However, this method is constrained by the acceleration of the movement in the discontinuity points of the toolpath. Similarly, Moetazedian et al. (2021) have studied the effect of filament retraction, the nozzle's traversal speed and acceleration on the shapes of the extruded beads as straight lines on both direct-drive and Bowden-tube hardware systems. Moreover, Wu et al. (2021) have presented linear and nonlinear control systems for synchronizing extrusion and motion control to enhance the precision of the extrusion process for CONVEX (CONtinuously Varied EXtrusion) models. Di Nisio et al. (2022) suggested using varying-width beads to create a porous infill structure. Changing the printing speed and extrusion rate during deposition produces thick and thin deposited sections. Although the nozzles with fixed circular orifices are capable of VBW printing, sophisticated geometries have not been fabricated yet in these works. A number of factors limit the success of these studies. Using extrusion/feed-rate modulation techniques, small circular nozzles can produce beads wider than their diameter. However, expanding the bead width beyond a limit presents unique challenges. Increasing pressure in the nozzle can cause leaks, material rebound, and nozzle clogging. Also, using large-size nozzles for thin bead widths may not be feasible with flow regulation techniques. Extruded material may exit the nozzle orifice without filling the chamber and with insufficient pressure. After dispersing at the edges, this material forms thick, poorly filled print traces with insufficient material supply.

The second approach necessitates a variation directly in the shape and size of the nozzle's outlet. The extrusion opening of the nozzle at the outlet is the ***orifice*** of the nozzle. In general, FFF is carried out via fixed-orifice nozzles. In the current state-of-the-art, functional mechanical solutions for achieving variable-orifice for the extrusion of thermoplastics are very limited. Instant nozzle shifts during manufacturing are also impractical. The second category itself can be divided into three sub-categories: (i) multi-extrusion systems, (ii) discretely and continuously variable cross-sections, and (iii) rotatable non-circular nozzles.

Multi-extrusion systems, i.e., extruding material through many nozzles of alternative sizes, allow for a wide range of possible BWs. However, the overall complexity of such systems increases due to the switching from one nozzle to another. Interrupting one nozzle from extrusion for switching to another is quite challenging (oozing may continue) (LaBossiere et al., 2009; Löffler and Koch, 2019).

Discretely and continuously variable cross-sections of the nozzles vary the widths of the extruded beads. However, they lead to delays when switching from one stage to another. In this category, one possible solution is multiple-stage nozzles to be driven by moving nested inserts inside the nozzle (Brooks et al., 2011). Continuously variable cross sections (Myerberg et al., 2018; Vanacker, 2017) bring greater printing flexibility with more possibilities for size changes during the fabrication of the artifacts. However, the majority of these designs are not easily realizable (or maintainable) due to their high geometric complexity and the overall manufacturing cost associated with them.

Rotatable non-circular nozzles with square-, rectangular-, and star-shaped orifices can extrude geometries of different shapes and sizes (Gharehpapagh et al., 2019). Nozzles with rectangular orifices cover a large interval of BWs by rotating the nozzle around its center. Lind et al. (2017) have patented

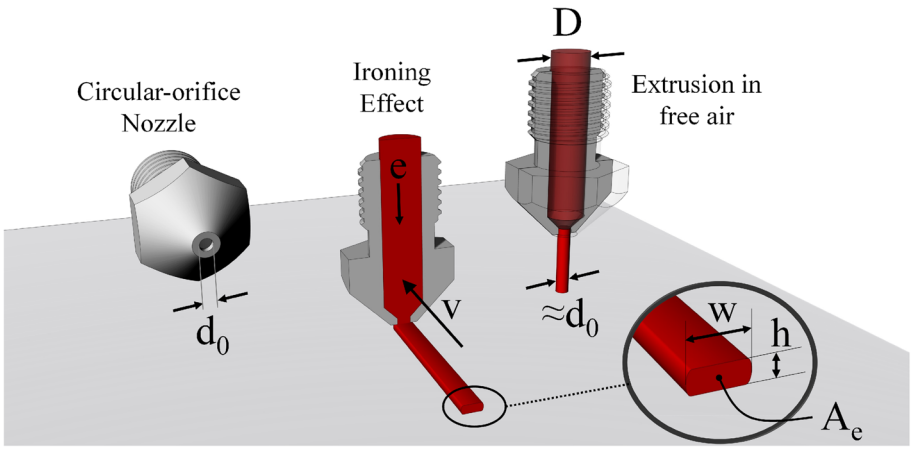

Fig. 1 Standard circular-orifice nozzle, geometry of extruded material after the ironing effect, and the extrusion in free-air

variable-width deposition in the field of Big Area Additive Manufacturing (BAAM), which allows for the printing of large-scale parts. They made use of a non-circular orifice to print VBW (Chesser et al., 2019). Xu et al. (2019) used a similar approach to extrude concrete to construct large-scale parts. Sculpman, a startup commercial enterprise (Vanacker, 2017), has presented a new extrusion system with a variable orifice whose opening can be controlled by a rotating mechanism while tracking the trajectory. Nevertheless, these concepts are still under development and have not yet been put into practice for FFF systems.

Another possible field of future research would be to investigate alternative extrusion systems for FFF. In this paper, a new extrusion system incorporating a rotatable nozzle with a non-standard opening without axial symmetry is introduced. The extrusion system is equipped with a rotating print head to steer the nozzle's oblong orifice in the programmed orientation. Thanks to the extraordinary design of the orifice, the effective dimension of the extrusion can be altered with rotational guidance. That implies a single rectangular-orifice nozzle functions as if the FFF is carried out by multiple nozzles. With this perspective, the developed system aims to attain variable bead width in FFF (or any MEAM processes) and alter the build resolution in distinct locations of the produced objects. The effectiveness of the designed extrusion system is evaluated through confirmatory test cases.

The outline of the paper is structured as follows: The next section introduces the theoretical foundation for the suggested concept as well as the extrusion system involved in realizing VBW in FFF. The used manufacturing platform and its subcomponents will be presented in detail. The third section elaborates on the fundamentals of necessary motion planning (i.e., how the rotational guidance of the oblong orifice will be managed) for obtaining desired BWs during FFF. The following section will explore the nozzle's flow characteristic, which is essential for optimizing the process parameters used in the experiments conducted. Next, the fifth section will show experimental evidence validating the potential of the proposed approach through a set of test cases. In the final section, the findings are to be wrapped up with some critical reflection and suggestions for moving forward in the future studies.

The variable bead width concept and the developed extrusion system

Classical FFF-type of 3D printers employ circular-orifice nozzles as the standard equipment for the extrusion of thermoplastics, as illustrated in Fig. 1. The orifice diameter (d_0) of commercially available nozzles (also known as nozzle size) ranges from 0.2 mm up to over 1 mm. With the standard equipment, the extruded material in a steady flow is shaped into the form of a continuously elongated cylindrical rod in free air. This is basically a reduction process in a hot chamber, where the large diameter of the solid filamentous material (D) is roughly scaled down to the size of the orifice ($\approx d_0$). For this process, the widely-used filaments are 1.75 mm and 2.85 mm in diameter. As long as the size of the orifice remains constant, the only way to adjust the diameter of the semi-liquid rod is to change the flow rate.

During FFF, these cylindrical rods are deposited onto the build plate or the surfaces of the existing layers. As a result, the round cross-section of the cylindrical rods turns out to be an elliptical shape due to the ***ironing effect*** imposed by the squeezing action of the nozzle. The ironing effect is described by the flattening of the extruded material between the nozzle's contact area and the base surface during the traversal of the nozzle. Hence, the round cross-section of the deposited material bulges and takes semi-circular shapes at both ends. The new dimensions of the flattened profile can be designated as the bead width (w) and the layer height (h). Note here that some insignificant details are disregarded in Fig. 1 for the sake of simplicity.

The FFF technology relies on the ironing effect to tailor the profile of the extruded material. In this way, the first prereq-

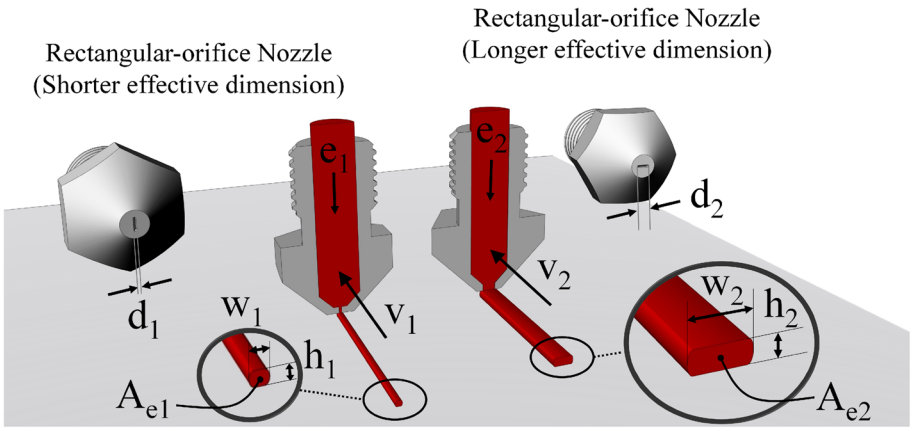

Fig. 2 (Left) Rectangular-orifice nozzle with shorter effective dimension (Right) Rectangular-orifice nozzle with longer effective dimension

uisite is to set the layer height lower than the nozzle diameter. That implies reduced layer height ($h < d_0$) together with an enlarged bead width ($w > d_0$) when compared to the size of the strand extruded in free air. The second condition is to regulate the extrusion rate (e) regarding the continuity of the material flow. Besides, the traversal speed of the nozzle must be synchronized with the extrusion rate to prevent under-extrusion or over-extrusion. Even if the optimal conditions are fulfilled, the BW can only be adjusted to some extent due to the viscosity of the extruded semi-liquid as it cools down. So, the applicability of this approach is restricted by the natural flow dynamics of the thermoplastics.

To offer a complete solution to realize the VBW concept, a novel idea is to alter the effective dimension of the orifice, as shown in Fig. 2. The following two important features of the proposed solution constitute the basic principle behind this method: (i) an axial asymmetry of the extrusion orifice, and (ii) the rotational degree of freedom of the asymmetric extrusion orifice. Figure 2 demonstrates the distinct cases while extruding thinner and thicker beads using the shorter (d_1) and longer (d_2) effective dimensions of the orifice, respectively. With the use of the orientation-controlled nozzle, a fast transition becomes possible between countless effective dimensions.

Design of the rectangular-orifice nozzle

One essential feature of the described method is to carry out the extrusion with an asymmetric orifice. Since the nozzles used in the existing FFF platforms are standardized (i.e., circular-orifice), custom-made nozzles have to be manufactured in the current investigation for the use in VBW printing.

In this study, the main extrusion unit mounted on the used FFF platform is a modified dual-extrusion Ultimaker print head. Thus, the design of the nozzle is such that it is compatible with an Ultimaker print core. Due to Ultimaker's user-friendly interface, the whole print core, including the custom-made nozzle, can be installed with little effort. This allows for seamless integration of the nozzle with the print head's temperature control components. In this setup, a Bowden tube extruder is available to force the filament (of 2.85 mm in diameter) through the nozzle with the use of a stepper motor and pushing mechanism comprising a set of gears.

The general structure and basic dimensions of the designed nozzle are similar to those of its standard counterparts, but the orifice is in the shape of a rectangular slot. In order to cover the range of widely-used nozzle sizes, the longer and shorter nominal dimensions of the orifice have been designed as 0.8 mm and 0.2 mm, respectively. FFF technology utilizes nozzles with diameters ranging from 0.2 mm to 0.8 mm. Nozzles with ∅0.4 mm are frequently preferred in general applications. Artifacts with fine/delicate features necessitate the nozzles with ∅0.2 mm (or smaller). However, the nozzles smaller than ∅0.2 mm (like ∅0.1 mm) are hardly ever used due to clogging problems encountered during operation. Tasks requiring very high build speeds utilize nozzle diameters up to 0.8 mm (0.6 mm is typical) at the expense of the introduction of stair-step effect along with the reduced dimensional accuracy. The proposed concept makes a synthesis of all these nozzle geometries:

- A rectangular nozzle driven along its short side (0.2 mm) emulates a fine-resolution nozzle;
- A rectangular nozzle driven along its long side (0.8 mm) acts as if a very coarse nozzle is employed;
- The effective area of the 0.2 mm by 0.8 mm rectangular nozzle (A) is

$$A = \frac{\pi(0.2\text{ mm})^2}{4} + (0.2\,mm \times 0.6\text{ mm}) \cong \frac{\pi(0.4\text{ mm})^2}{4}.$$

This approximately corresponds to the area of a conventional circular nozzle with a diameter of 0.4 mm. Note that this diameter is extremely popular in the FFF technology due to its operational simplicity.

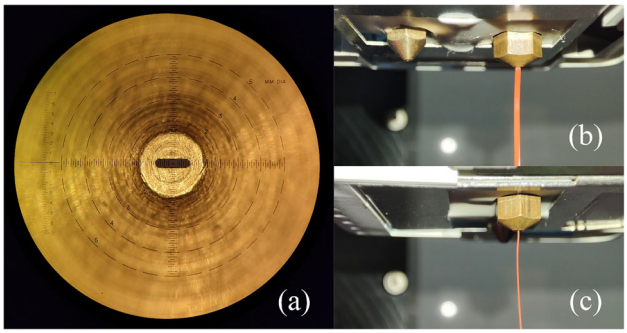

Fig. 3 **a** Magnified view of the outlet orifice, **b** The view of the extruded beads with the longer dimension of the orifice, **c** The view of the extruded beads with the shorter dimension of the orifice

The manufacturing of the rectangular opening has been carried out on a waterjet-guided laser system by Synova SA. Brass, which is the most typical material for the body of an FFF nozzle, was used in the construction of the nozzle. The magnified view of the produced rectangular-orifice nozzle is shown in Fig. 3a.

As a natural consequence of the cross-sectional profile, the extruded beads take a rectangular shape whose longer and shorter edges are visible in the free air, as shown in Fig. 3b and c, respectively[1]. That gives the rough shape of the extruded beads and contributes to extra thickening or thinning right before the ironing.

Fused filament fabrication platform

The nozzle designed for use in VBW applications must also have a rotational degree of freedom (DoF) for controlling the effective dimension of the extrusion orifice. Thus, in order to realize the proposed method, an FFF platform with a minimum of four motion axes is required. Although the attachment of an extra rotational axis to a standard (i.e., 3-axis) FFF platform may be considered a cost-effective option, the mechanical structure of such systems is generally not suitable for modifications. In this study, a unique multi-axis platform that was originally designed for hybrid manufacturing is to be utilized. Two main functions of the manufacturing platform (as shown in Fig. 4) can be summarized as follows:

- Additive Manufacturing through the use of Q-W-X-Y-B-C kinematic chain, and
- Subtractive Manufacturing through the use of Z-X-Y-B-C kinematic chain.

In VBW printing applications, the X, Y, and W linear axes (or the rotational C-axis as well) are used to position the print table with respect to the extrusion nozzles. Besides, the rotational Q-axis serves the purpose of controlling the orientation of the nozzle's orifice.

The main extrusion unit, the dual extrusion Ultimaker print head, is attached on the Q-axis of the machine. There have been two separate connection interfaces for Ultimaker print cores in the main extrusion unit. The placement of the rectangular-orifice nozzle is carried out such that the vector passing through the origin of the orifice coincides with the rotational Q-axis, as shown in Fig. 4. The main extrusion unit can be rotated without restriction as long as the wires and filament tubes are not excessively twisted. For a secure motion without any twisting problems, the rotation of the Q-axis is set in the range of $[-2\pi, 2\pi]$ interval.

Dynamic control of nozzle rotation via Q-axis

The trajectory of the main extrusion unit can be characterized as a discretized 2D curve after slicing a 3D artifact. That is, the path is conveniently represented as an ordered set of points:

$$\boldsymbol{P} = \{\boldsymbol{p_n} = (x_n, y_n) \in \mathbb{R}^2 : \quad \forall n \in \mathbb{N}_{\leq N}\} \tag{1}$$

where N refers to the total number of base points in the set[2]. For the special nozzle discussed here, the orientation of the main extrusion unit (and obviously the nozzle) should be controlled to attain the desired BW by taking into account the tangents of the trajectory. For a constant BW, the Q-axis angles[3] can be specified as an ordered set as well:

$$\boldsymbol{\Theta} = \left\{\theta_n \in [-\pi, \pi] : \theta_n = \tan^{-1}\left(\frac{y_{n+1} - y_n}{x_{n+1} - x_n}\right) + \theta_0 : \quad \forall n \in \mathbb{N}_{\leq N}\right\} \tag{2}$$

where θ_0 stands for the initial angle specifying the desired BW. In fact, the angles $(\pi/2 < \theta_n \leq \pi) \vee (-\pi \leq \theta_n < -\pi/2)$ do not have any physical meaning in this configuration owing to the fact that when $-\pi/2 \leq \theta_n \leq \pi/2$, an arbitrary trace could be laid in any quarter of the plane. Hence, the set defined in Eq. (2) can be remapped:

$$\boldsymbol{\Theta^*} = \left\{\theta_n^* \in [-\pi/2, \pi/2] : \theta_n^* = \theta_n - \pi H\left(\theta_n - \frac{\pi}{2}\right) + \pi H\left(-\theta_n - \frac{\pi}{2}\right) : \quad \forall n \in \mathbb{N}_{\leq N}\right\} \tag{3}$$

[1] The supplementary video of Fig. 3b and c is given as: https://youtu.be/FFQcj651lno

[2] In this study, 0 is excluded from the natural numbers.

[3] The rotary extruder head used in the experimental study does not have a slip ring to allow infinite rotation around its axis. Furthermore, the filament fed through the extruder head imposes a mechanical torsional limit. The rotation of the Q-axis is to be restricted to a full turn in both directions (CW/CCW): $-2\pi \leq \theta_n \leq 2\pi$.

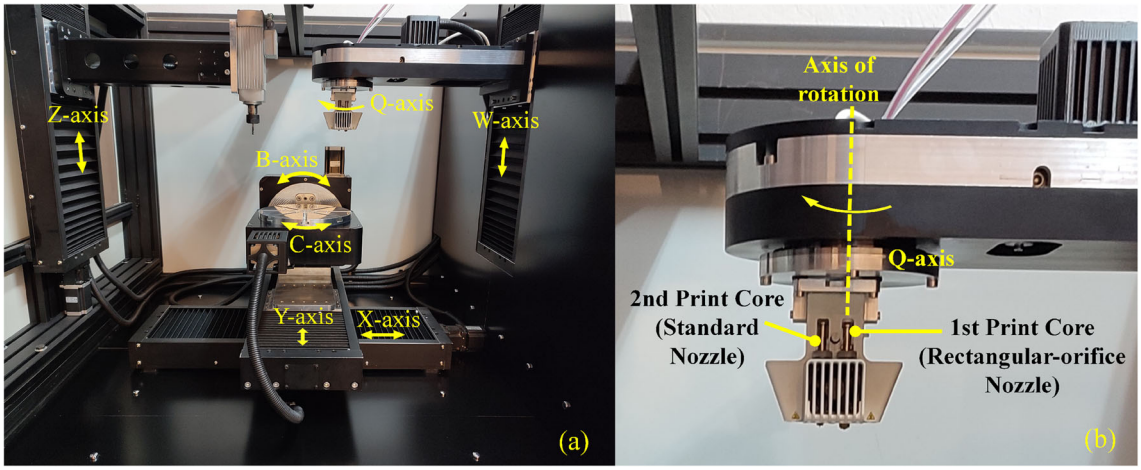

Fig. 4 The used machine setup **a** motion axes, **b** details of the main extrusion unit

where H refers to the Heaviside existence function:

$$H(x) = \begin{cases} 1, & x \geq 0, \\ 0, & x < 0. \end{cases} \tag{4}$$

Note that the relation between θ_0 and the desired BW can be given as

$$w = d_1 \cos(\theta_0) + d_2 \sin(\theta_0) \tag{5}$$

where d_1 and d_2 are the dimensions of the short- and long side of the nozzle's cross-section (assuming the profile as a perfect rectangle). Hence, the initial rotation can be expressed in terms of the desired bead width, i.e., $w \in [d_1, d_2]$:

$$\theta_0 = 2\tan^{-1}\left[\frac{d_2 \pm \sqrt{d_1^2 + d_2^2 - w^2}}{d_1 + w}\right] \tag{6}$$

It is self-evident that variable bead width can be obtained by continuously adjusting θ_0 using Eq. (6). Likewise, in order to maintain a constant bead width (thus, θ_0 remains constant), θ_n must always be updated for every point n on the followed trajectory. The latter condition is more likely to take place, since the sudden change in the BW is not the main focus of this study. Figure 5 provides a visual representation of the aforementioned condition by demonstrating the four distinct orientations of the θ_0's that correspond to the four different target BWs on the same trajectory. Here we see, from the top view, how the cross section of a perfect rectangular nozzle looks as it passes through a series of points on the trajectory. Therefore, the final shape of the extruded strands can be estimated by integrating them over those points.

The remapped (or wrapped) angles in Eq. (3) do have some serious consequences on the fabrication performance since the nozzle carries out 180°-sweep at each angle transition

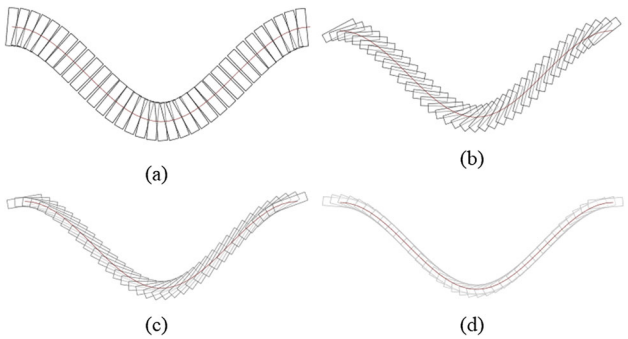

Fig. 5 A trajectory extruded via rectangular-orifice nozzle with four different values for w and θ_0 as **a** $w = 0.8$ mm and $\theta_0 = 90°$, **b** $w = 0.6$ mm and $\theta_0 \approx 32.4°$, **c** $w = 0.4$ mm and $\theta_0 \approx 14.4°$, and **d** $w = 0.2$ mm and $\theta_0 = 0°$

(either from 90° to -90° or -90° to 90°). The mathematically constrained operating range of the Q-axis is practically expandable up to the mechanical limit (due to the existence of multiple equivalent solutions to the problem).

$$\boldsymbol{\Theta}^{**} = \left\{\theta_n^{**} \in [-2\pi, 2\pi] : \theta_n^{**} = \theta_n^{*} \pm k\pi : k \in \mathbb{Z} \quad \forall n \in \mathbb{N}_{\leq N}\right\} \tag{7}$$

That is, with the best selection for the parameter k in Eq. (7), a large interval up to the mechanical limits of the used platform can be utilized, i.e., two full turns. Still, some strategies must be devised to minimize the effects of any possible swings on the trace, in case the tool path makes it inevitable to go beyond the mechanical limits. To avoid oozing, one possible strategy for such transitions is to retract the filament and optionally move the nozzle up.

Another restriction is the possible high-curvature regions encountered along the traced paths. Since the orifice is rectangular in cross-section, the smoothness of the extrusion width can be degraded, and bulging occurs along the path if there

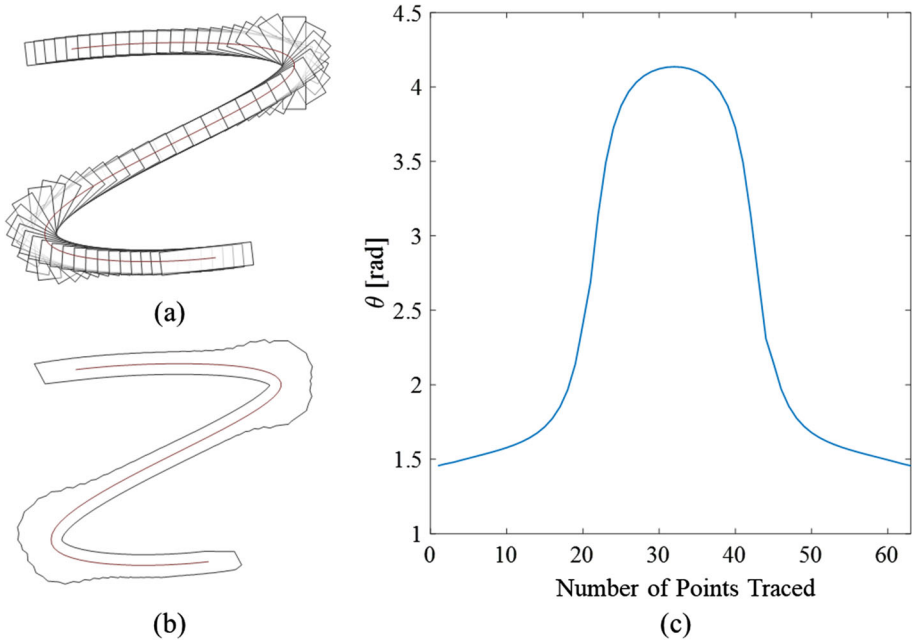

Fig. 6 A sample trajectory traced by the proposed nozzle **a** discrete locations of the nozzle **b** expected overall shape **c** the necessary angles along the way

exist sudden changes in the derivative of the rotational angle. This is much more pronounced, especially when a smaller effective dimension is on duty. Figure 6a illustrates a sample trajectory with sharp turns and the nozzle geometry as it passes through individual points. The resultant extrusion quality along the path is deteriorated, as inferred from Fig. 6b. This can also be expected due to the sudden changes of θ_n at respective locations (Fig. 6c). For such challenges, a suitable path planning strategy or extra flow management should be applied. For instance, doing evasive maneuvers (back and forward) along the path by preprocessing the topology may be a suitable option as well as the controlled flow in those critical points. However, since that is not the main topic of our paper, we do not get into those specific details here.

Flow characteristics of the nozzle having rectangular-orifice

In theory, when employing a rectangular orifice with varying sizes and aspect ratios, the fundamental equation essential for flow analysis is the continuity equation. When extruding in free-air under normal conditions, all the material entering the hot nozzle exits, allowing for the straightforward determination of the resulting cross-sectional area of the outlet strand. However, during the actual process of layering in 3D printing, there are a wide variety of elements that can affect the flow. These effects stem from the reasons like the pressure distribution at the nozzle exit due to an asymmetrical cross-sectional profile, or errors inherent in the entire extrusion system. To comprehensively analyze the flow of a generic rectangular-orifice nozzle applicable in real-world scenarios, one must scrutinize the impact of numerous parameters in each conceivable configuration. Nonetheless, achieving this necessitates the creation of diverse nozzle geometries, conducting tests across various parameters, and formulating a methodology as an outcome.

In this section, the emphasis is not on examining the flow characteristics of a generic rectangular-orifice nozzle; rather, the goal is to make the requisite adjustments tailored to the nozzle designated for our experimental use. Furthermore, Appendix A provides insights into certain factors that may require consideration when fine-tuning the flow for a generic rectangular-orifice nozzle.

To get the best print quality, it is essential to have a clear understanding of the specific flow characteristics of the customized nozzle. The free-shape and ironed dimensions of the extruded strands can obviously be affected by a number of factors, including (i) extrusion flow rate, (ii) nozzle traversal speed, (iii) layer height, and (iv) melt pool temperature. Based on the results of the preliminary trials, the major emphasis will be on the first two factors due to their greater impact compared to the others. Firstly, it is necessary to clarify the ideal operation range for the extrusion flow rate that the custom nozzle can handle. Secondly, the contribution of the nozzle's traversal speed to the fine-tuning of the BW is to be explored. Both of these crucial factors need to be in harmony with one another. Otherwise, leakage or any blockage of the nozzle may happen due to the unmanageable rise in the internal pressure of the nozzle's melt pool. Also, the extruder may have difficulty keeping up with the unsynchronized traversal speeds, i.e., slipping of the filament with respect to the forcing gear. The remaining factors will be briefly addressed in the last part of this section.

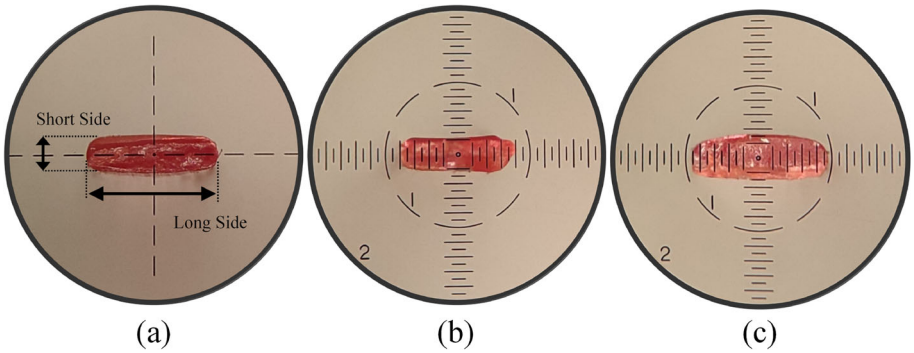

Fig. 7 **a** Cross-section of the extruded material in free-air, **b** Cross-section of the extruded material obtained at $e = 0.1$ mm/s, **c** Cross-section of the extruded material obtained at $e = 1$ mm/s

The BW control method proposed in this work relies on manipulating the effective dimension of the orifice to achieve the desired rough form of the extruded cross-sectional profile. Then, the ironing effect often contributes to a slight enlargement of this profile on the built plane while maintaining a stable layer thickness on the traversed path. Without the ironing effect, the extruded geometry resembles the general form of the oblong extrusion orifice. Figure 7a shows the micrograph of the cross-sectional profile extruded in free-air. Evident from the respective dimensions shown in Fig. 7b and 7c, the extruded profile expands as a result of a higher flow rate. This implies that the flow rate management allows for optional manipulation of the rough dimensions (i.e., short- and long-sides). Nevertheless, forcing the overflow or underflow for BW control has not been the focus of the current research. So, this section serves the sole purpose of exploring the range of the optimal flow settings that will be employed in the test cases later on.

With this aim, the custom nozzle has first undergone testing to determine a stable range of flow that prevents it from leaking or becoming blocked and the filament from slipping with respect to the extruding gear of the Bowden tube filament feed mechanism. Once an appropriate range for consistent and steady extrusion has been found, the fine-tuning for achieving the desired BW has been examined thereafter, by searching for the optimum nozzle traversal speed.

Figure 8 illustrates the relation between the extrusion flow rate and the observed dimensions during extrusion in free-air. At any flow rate, the blue and red trendlines can be used to predict the dimensions of the long and short sides, respectively. A flow rate between 0.05 mm/s and 1 mm/s is set as the suitable operating range for a number of reasons. First of all, this range covers the necessary flow rate corresponding to the maximum traversal speed of the nozzle achievable by the manufacturing platform. Also, the flow of the material is stable in this range, where under-extrusion or over-extrusion rarely exist both before and after the ironing effect. In fact, the custom-made nozzle can even handle a flow rate well above 2 mm/s if there is no other resistance to the flow (in free-air).

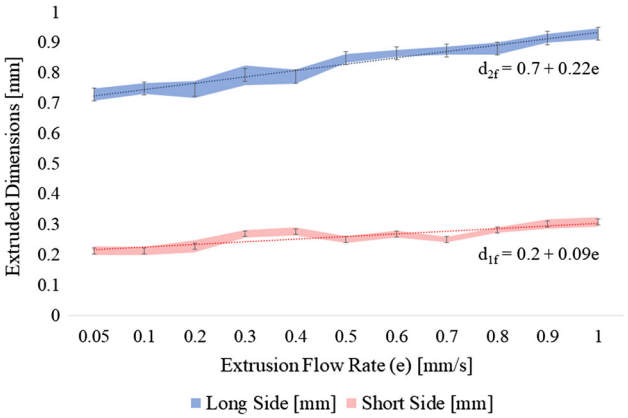

Fig. 8 The flow characteristics in free-air

Ignoring the time lag caused by the Bowden tube extrusion mechanism, the extrusion flow rate is directly proportional to the nozzle's traversal speed. The following expression provides the relation based on the conservation of the volume:

$$e = \frac{A_f}{A_e} v \tag{8}$$

In Eq. (8), e and v denote the rates at which the extruder gear feeds the material and the velocity with which the nozzle travels with respect to the build plate, respectively. The area of the filament cross-section, denoted by A_f, is known in advance thanks to the fixed diameter of the filament ($D = 2.85$ mm). On the other hand, the cross-sectional area of the extruded profile, A_e (see Figs. 1 and 2), is a floating quantity due to the following reasons: (i) It is dependent on the expected BW, which is a function of the effective dimension of the orifice, (ii) The extruded profile is not a definite shape such as a perfect rectangle.

Hence, the variation in the cross-sectional area of the extruded profile is simply modeled as follows:

$$A_e(\theta_0) = c_f h w(\theta_0) \tag{9}$$

In Eq. (9), h refers to the constant layer height maintained after the nozzle's ironing action. The given equation asserts

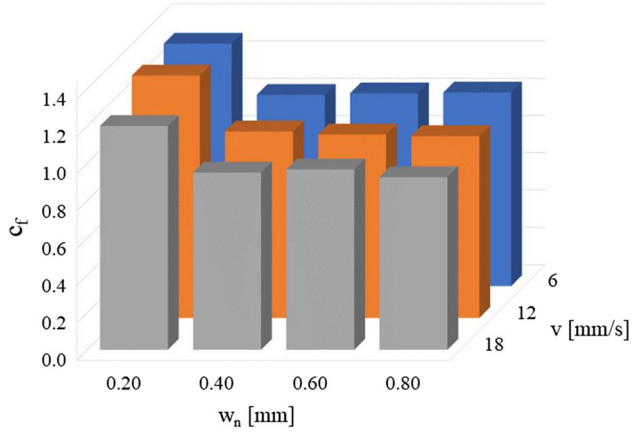

Fig. 9 The compensation factor at various traversal speeds during extruding desired nominal BW at different initial angles

that the variation in the cross-sectional area is governed by the initial angle of the oblong orifice denoted by θ_0. This implies that dynamic control of the nozzle's rotation alters its effective dimension, which then modifies the bead width designated as w. (Refer back to the set of equations for a reminder on how dynamic control of the nozzle's rotation is applied.)

It is worth mentioning that the area A_e is not simply computed by multiplying the layer height h by the bead width w, since the ultimate cross-section of the profile (i.e., deposited and cooled after the ironing action) cannot be thought of as a perfect rectangle. To account for any expansion or contraction, a compensation factor represented by c_f in the Eq. (9) is utilized. This factor is largely influenced by the nozzle's traversal speed.

In order to get the compensation factors shown in Fig. 9, certain experiments are conducted within a range of nozzle traversal speeds. The compensation factors c_f are calculated as the ratio of the actual bead width obtained in those experiments to the nominal bead width desired. Apparently, the expected BW and the achieved BW are identical if the factor is unity. Therefore, to achieve optimal outcomes in the upcoming test cases, we should use traversal speeds where c_f is close to 1. According to the data presented in Fig. 9, the best traversal speed of the nozzle is around 10 mm/s for a wide spectrum of BWs, with the exception of the minimum one. Accordingly, we have settled on this traversal speed for our forthcoming tests. Moreover, a minimum of 0.2 mm bead width cannot be achieved even with the 18 mm/s traversal speed of the nozzle. Thus, if we target a 0.2 mm bead width, we will use a compensation factor of 1.2–1.4, which will bring the minimum achievable BW up to 0.25–0.28 mm.

In this study, the temperature of the nozzle is set to 205 °C for the extrusion of PLA material, as recommended by the filament manufacturer. Also, the maximum layer height is considered to be half of the specified BW in the experiments. In summary, many parameters have been examined and determined for their appropriate amounts in this section. Table 1 displays the results of the analysis, in which the optimal values for numerous parameters are established. Unless otherwise specified, the chosen set of parameters is employed in all of the test cases in the next section.

Table 1 Process parameters used in the experiments

	Process parameters	Selected value
Operational	Material flow rate [mm/s]	0.1–1
	Layer height [mm]	$\leq w/2$
	Filament material	PLA
	Temperature [°C]	205
Motion	Nozzle traversal speed [mm/s]	10
	Maximum Q-axis rate [rad/sec]	2.5
Nozzle	Minimum effective dimension, d_1 [mm]	0.2
	Maximum effective dimension, d_2 [mm]	0.8
	c_f (if the minimum BW targeted)	1.2–1.4
	c_f	1

Results and discussion

The novel feature of the proposed method is its functionality in adjusting the (i) intralayer and (ii) interlayer build resolutions. The former term refers to altering the bead width during extrusion on a layer, while the latter indicates adapting the layer height during stacking of them. This section will show experimental evidence for the potential of the proposed approach in customizing the interlayer/intralayer build resolution in a variety of contexts and assisting the FFF process as if it were carried out with multiple nozzles. Table 2 provides a concise summary of the experimental test cases along with the associated types.

Modification of the BWs within the layers is the subject of the first two test cases listed; the first one provides experimental confirmation of the VBW concept, while the second test is designed to evaluate how well the concept holds up in practice. Similarly, the third test case presents the simplest validating illustration of the stacked layers with different heights, and the fourth one serves as a benchmark highlighting the advantages of the proposed method over the traditional FFF approach.

Test Case #1: Variable Bead Width

To demonstrate the proof of the concept, the first test case is designed to visualize the variations in the bead width (in a pair of parallel experiments). Experiment 1a and Experiment 1b are conducted to realize the same goal, where single-wall extrusions with VBW are targeted along a circular and a linear path, respectively. In these experiments, the effective

Table 2 The summary of the conducted experiments

Test case		Type	Summary
#1	Variable bead width	Intralayer	Aim: obtain constant BWs for discrete effective dimensions of the nozzle
			Result: BWs of 0.28 mm, 0.40 mm, 0.60 mm, and 0.80 mm dimensions
#2	Adjoining clubs		Aim: obtain constant BWs while tracing along a complex path
			Result: Thin (0.28 mm) and thick (0.8 mm) BWs printed on the same path
#3	Adaptive layers	Intralayer + Interlayer	Aim: obtain adaptive variation of the layer height
			Result: A wall with variable build resolution in discrete local sections
#4	Vase		Aim: obtain a benchmark case, comparison to the standard approach
			Result: 3D structure with both VBW and adaptive layers

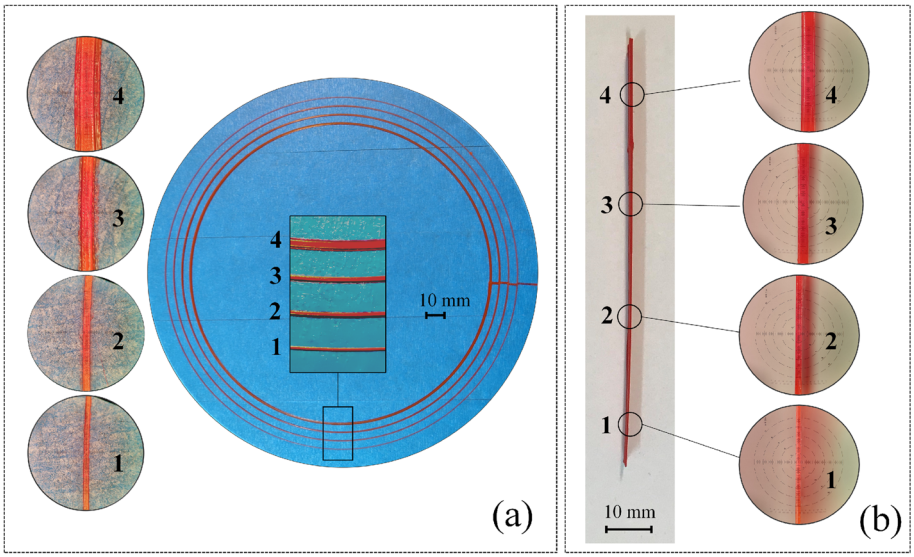

Fig. 10 Top view of the walls extruded as single lines of VBW

dimensions caused by the discrete orientations of the nozzle play the main role in adjusting the BW.

Here, it's worth remembering that the nozzle's effective dimension varies depending on the angle at which its oblong orifice is positioned relative to the surface on which the material is being extruded. Equation (5) shall be used to get the feasible angles, while Eqs. (8) and (9) are useful to compute the necessary quantity of the material.

Experiment 1a is made with the intention of exploiting the nozzle's four discrete effective dimensions, in which a series of constant BWs are extruded as concentric circles, as shown in Fig. 10a. Each circle is made by stacking uniform layers of 0.1 mm height, with BWs of 0.28 mm, 0.4 mm, 0.6 mm, and 0.8 mm. During the experiment, the C-axis is responsible for the relative motion between the nozzle and the build table (see Fig. 4), so the Q-axis is held steady and inactive in its discrete orientations. Table 3 presents the angles and the accompanying nominal BWs that were sought after using the aforementioned set of equations.

Experiment 1b is carried out in a similar fashion, but while traveling in a straight line this time, as shown in Fig. 10b. Layers of 0.1 mm height are extruded on top of each other while the machine moves along the X axis, aiming for the identical BWs as in Experiment 1a.

Table 3 The Q-axis angles set for accompanying nominal BWs and the observed BWs in the experiments

#	θ_0	Nominal w [mm]	Experiment 1a w [mm]	Experiment 1b w [mm]
1	0°	0.28	0.26	0.25
2	14.4°	0.40	0.40	0.40
3	32.4°	0.60	0.60	0.60
4	90°	0.80	0.84	0.80

According to the preliminary results summarized in Table 3, both experiments show acceptable outcomes thanks to the use of discrete initial angles and synchronized extrusion rates predetermined by the given equations. In fact, with some additional fine-tuning, the desired nominal BW can also be precisely attained and maintained along such simple tool trajectories.

Test Case #2: Adjoining Clubs

Experiment 2 is designed to evaluate how well the VBW concept holds up in practice. The main goal of the second test case is to maintain a constant BW as an intricate path is traveled, which obliges actively maneuvering the nozzle's oblong orifice considering the tangents of the path. That is, for every point on the path represented by an ordered set in Eq. (1), the Q-axis must be continuously rotated in accordance with the angle determined by the corresponding equations.

In order to evaluate how well the suggested method works in a realistic and hard scenario, we choose a club-shaped path including sharp turns on the trajectory, as shown in Fig. 11a[4]. In this scenario, it is aimed to demonstrate two different BWs (the maximum and minimum ones) that the nozzle can extrude on the planned path. Thus, by using filaments of distinguishable colors, the clubs that are adjacent to one another but have different BWs are deposited in separate fabrications and then grouped together. The intended nominal BWs are 0.28 mm and 0.8 mm for the clubs manufactured with red and black filaments, respectively. It is inevitable, however, that dimensional errors may occur due to the sharp turns on the path, similar to the case presented in Fig. 6.

To illustrate the achieved performance, measurements of the BWs are taken at various locations distributed along the polar coordinates of the test piece, as shown in Fig. 11b. The red points show the most dangerous spots because the Q-axis has to move quickly to deal with the high curvature there.

For the mapping of the errors along the path, the measured BWs are normalized by the desired nominal BW values for every measurement spot. Here, the ratio of the measured BW to the desired nominal BW stands for the relative percentage.

Three repetitions of each print were made to analyze the reproducibility of the output. The results of the total of six tests (three for the thinner/red, three for the thicker/black) are provided in Fig. 11c. The results have shown that unwanted thickening of the BW (up to 150%) was observed at the critical spots where fast turns of the Q-axis are experienced. The rapid rate of change of the Q-axis movement (shown in Fig. 11d) provides more evidence for the expected thickening at the sharp turns. The ratio is close to 100% everywhere except the areas of extreme curvature, showing that the desired BWs can be attained with high accuracy at those measurement points.

Test Case #3: Adaptive Layers

It has been noted before that the maximum attainable layer height increases in FFF as the nozzle size grows. Applying this justification to the VBW concept, it becomes clear that a nozzle with a variable effective dimension allows for flexible layer heights during production, i.e., a direct impact on the build resolution.

According to the rule of thumb that the layer height should be less than half of the nozzle size, the maximum practical layer height is 0.4 mm, given that the biggest effective dimension of the used nozzle (d_2) is roughly 0.8 mm. Although there is no hard limit on how thin the layer can be, we typically aim for a minimum of 0.05 mm layer height for not to slow down the production too much.

Figure 12 displays a prototype wall that was fabricated employing alternative build resolutions for separate regions[5]. Section 1 of the wall has been produced by stacking straight lines of 0.2 mm layer height and 0.8 mm bead width. Similarly, layers of 0.05 mm with 0.26 mm bead width have been deposited to create Section 2. The magnified views depict the noticeable difference in the appearance of the discrete sections fabricated with alternative build resolutions. It is therefore verified that both the bead width and the layer height can be flexibly controlled in separate local regions of an object manufactured by the proposed method.

Test Case #4: Vase

The final test case will serve as a benchmark against which the suggested method is to be evaluated and compared to the standard FFF approach. A vase-like object is to be flexibly manufactured with varying layer heights and BWs at its distinct sections. It is remarkable because the conventional FFF method calls for employing three different-sized nozzles (small, medium, and large) to do the same task that a single nozzle did in our platform.

The vase is conceptualized and manufactured with three distinct sections, each with its own unique layer height and BW, where the designed parameters are detailed in Table 4.

Figure 13 depicts the process of making the vase-shaped object from start to finish and its final view in an illuminated environment[6]. The nozzle's placement along the extrusion route has been accomplished using the X, Y, and Z-axes, while the Q-axis is continuously rotated to maintain the nozzle's rectangular-orifice at the computed angle.

The proposed extrusion technology makes it simple to create the vase-shaped object. Nevertheless, the conventional FFF method, which involves employing a single pre-selected nozzle in the process, is practically incapable of production with typical nozzle sizes (0.4 mm and above). Indeed, the current design specifications can only be fulfilled by using the smallest available nozzle size for the standard FFF approach (i.e., ≈ 0.25 mm), but at the cost of a significantly long production time. Thus, it is useful to examine the suggested approach's performance against that of the standard FFF method through a few representative scenarios.

[4] The supplementary video of Fig. 11a for the red part is given as: https://youtu.be/kx5xKTvOvXw

[5] The supplementary video of Fig. 12 is given as: https://youtu.be/qmoEqY687Os

[6] The supplementary video of Fig. 13 is given as: https://youtu.be/Q7pIwVarev8

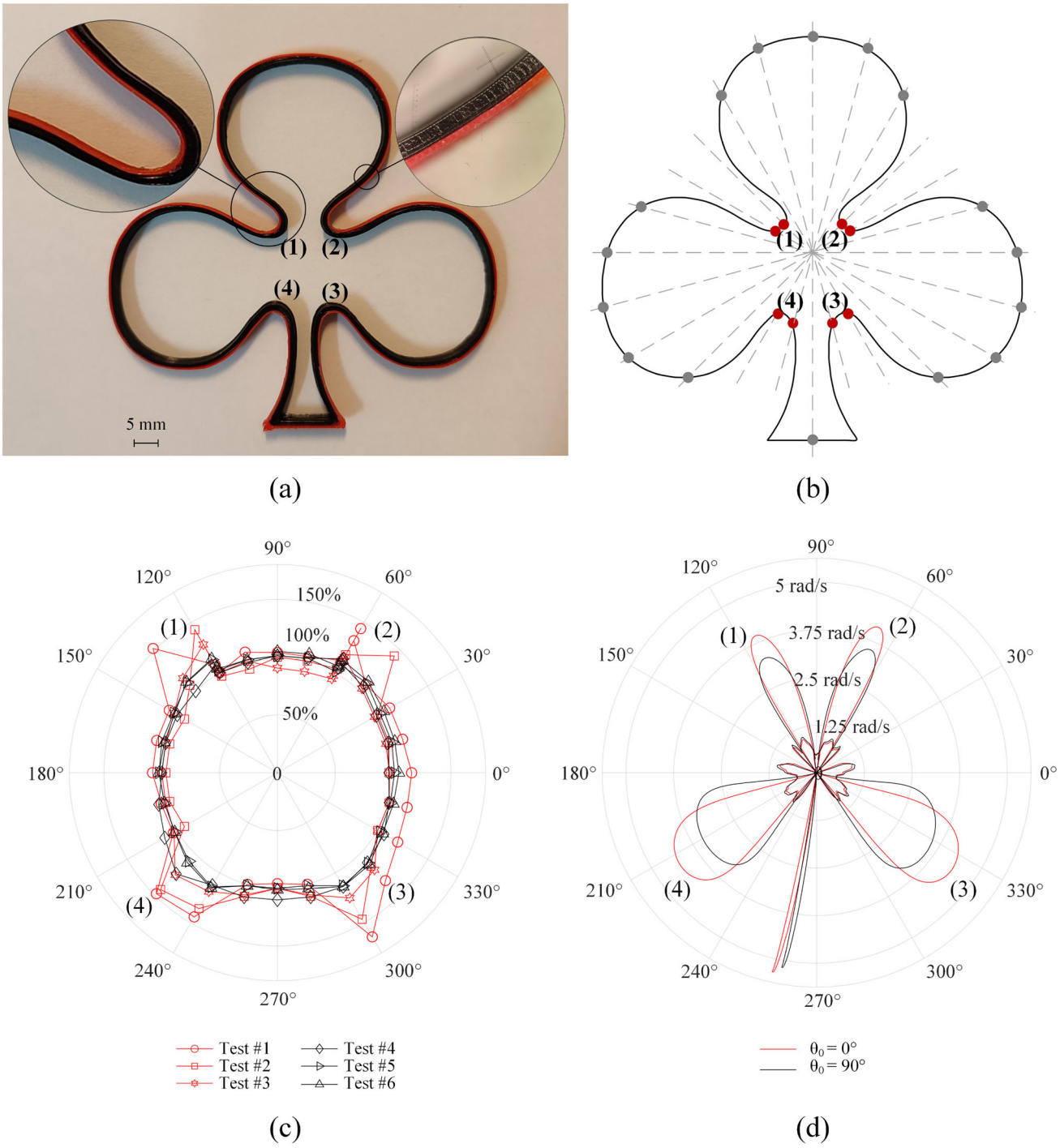

Fig. 11 Club-shaped shells and **a** their extruded parts, **b** illustration of selected points through the trajectory in error map, **c** error map where Tests 1, 2, and 3 are for the outer shell and Tests 4, 5, and 6 are for the inner shell, and **d** Q derivatives through trajectory

Three distinct scenarios are generated to compare the performance in terms of production quality and build time. The details of them are set forth in Table 5, along with the theoretical comparison of the expected build time. These scenarios demonstrate how different-sized nozzles (available for an Ultimaker print core) may simulate fine, medium, and coarse build resolutions in the process. In addition, we allow for a flexible tuning of the BW within a closed range of the nozzles' diameters, as a fair assumption for circular-orifice nozzles.

We can confidently predict the best possible product quality in the first scenario, since the used nozzle offers the finest

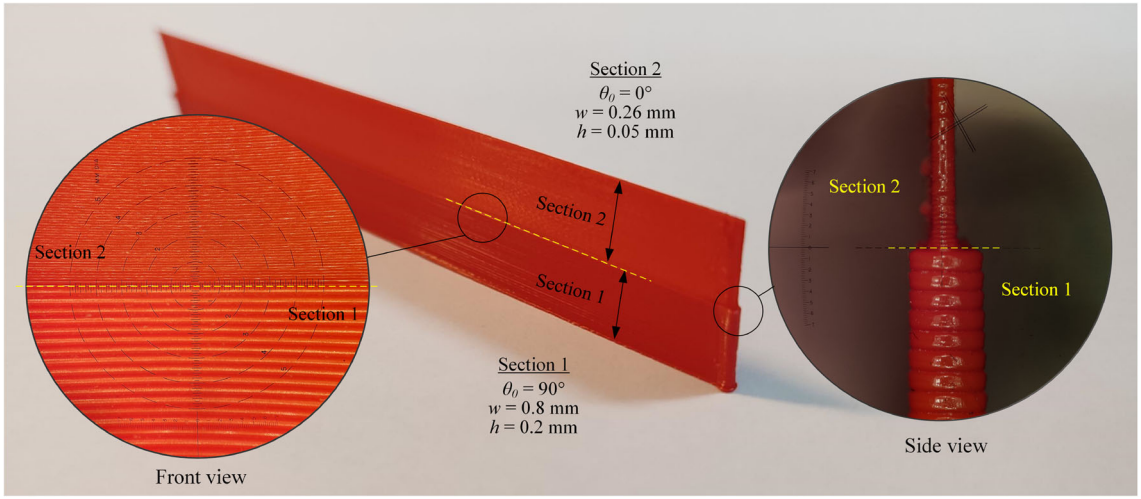

Fig. 12 A wall built with two kinds of bead sizes and layer thicknesses

Table 4 Design specifications for the individual sections of the vase part

Section #	w [mm]	h [mm]	Number of layers	Total height [mm]
1	0.8	0.2	300	60
2	0.4	0.1	300	30
3	0.25	0.1	300	30

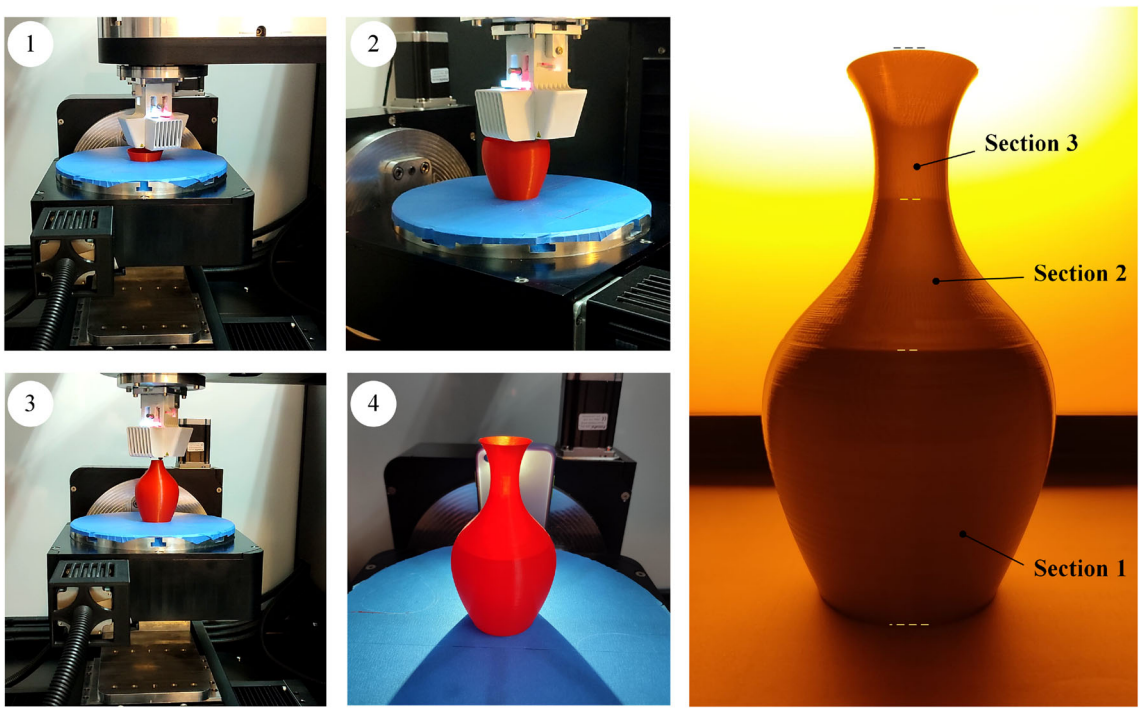

Fig. 13 A vase as a test case fabricated with three different sections via rectangular orifice-nozzle

Table 5 Comparison of the proposed method with the scenarios for circular-orifice nozzles with different sizes

Design specification for Vase's sections			Scenario 1: $d_0 = 0.25$ mm standard nozzle		Scenario 2: $d_0 = 0.4$ mm standard nozzle		Scenario 3: $d_0 = 0.8$ mm standard nozzle		Proposed method: $[d_1, d_2]$ = [0.2 mm, 0.8 mm]
#	h [mm]	w [mm]	Possible options repetition*×(w)**	Build time [min]	Build time [min]		Build time [min]		Build time [min]
1	0.2	0.8	2×(4×0.20 mm)	600	☒		☒		75
			2×(2×0.40 mm)	☒	300		☒		
			2×(1×0.80 mm)	☒	☒		150		
2	0.1	0.4	1×(2×0.20 mm)	86	☒		☒		43
			1×(1×0.40 mm)	☒	43		☒		
3	0.1	0.25	1×(1×0.25 mm)	25	☒		☒		25
Overall build time				711	N/A		N/A		143

*Since uniform slicing is assumed in these scenarios, Section 1 requires twice repetitions of the 0.1 mm layers. (2×0.1 mm = 0.2 mm)
**The overall bead width can be assumed as the total width of the union of separate adjoining lines. (4×0.2 mm = 0.8 mm)

build resolution. But, it is necessary to make a serious sacrifice in the overall build speed. If the objective is to produce a thick (0.8 mm) BW with the smallest nozzle, for instance, it is unavoidable to unionize a bunch of extruded lines, which slows down the process of making an identical layer by a factor of four. Likewise, it is necessary to make multiple repetitions to manufacture equally thick layers when the target layer height is not attainable by the utilized nozzle. In other scenarios, the bigger nozzles might not be capable of printing BW as thin as 0.25 mm, which would result in a total manufacturing failure. In comparison, the proposed approach has the advantage of producing with the fastest build speed and succeeding in all conditions described in the design specifications of the vase.

Just as in the theoretical comparison outlined above, it is also useful to undertake the production on a typical 3D printer using the conventional FFF pipeline to analyze the final product quality. For this purpose, we use an Ultimaker 3 Extended to produce the vase-shaped object, where the printing parameters and the tool path are determined using the commercial slicing software, Cura.

It is preferred to carry out the production with the 0.4 mm nozzle, because the smallest available nozzle for an Ultimaker print core (i.e., 0.25 mm) frequently clogged in the trials. The extrusion parameters used in the commercial software are quite close to those employed in our machine, except for the bead width. Alternative bead widths (known as line width in Cura) are examined, and the end products manufactured on the Ultimaker 3D printer are shown in Fig. 14. Note here that the commercial software sometimes fails to provide a slicing option with the required BW.

In the actual tests, we produced the red part in 143 minutes, while the white parts were completed over much longer durations on the Ultimaker. Under-extrusion problem or even a total failure are likely to occur with the standard FFF approach, as seen from the poor quality of the products in Fig. 14b and c.

Conclusion and future work

FFF comes with the trade-off between the build speed and the output quality. The extrusion nozzles are mostly responsible for the finite build resolution inherent to the FFF process conducted by the standard pipeline.

In the current state-of-the-art, alternative methods exist to modify the build resolution: (i) replacement of the nozzle with a different-sized counterpart, (ii) flow management without the replacement of the nozzle, (iii) other innovative technologies that enable dynamic nozzle size changes.

The first alternative is impractical with the current processing pipeline, and the second has restricted potential due to the nature of thermoplastics. That leaves dynamic adapta-

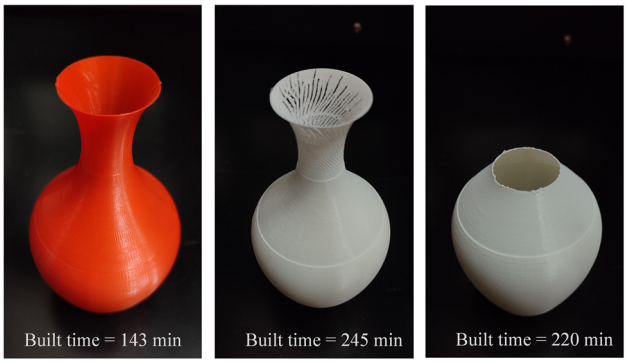

Fig. 14 The vase test case manufactured by **a** the proposed rectangular-orifice nozzle **b** circular-orifice nozzle using $w = 0.25$ mm and $d_0 = 0.4$ mm **c** circular orifice nozzle using $w = 0.8$ mm and $d_0 = 0.4$ mm

tion of the nozzle size in the process as the best option, but it is rarely achievable without using cutting-edge technologies.

The proposed method offers a smart solution for in-process alteration of the nozzle size (referred to as the effective dimension previously). A rectangular-orifice nozzle, the alignment of which must be constantly guided, is the key to achieving this. From this point of view, the proposed method has the potential for both dynamically varying intralayer build resolution (i.e., variable bead width) and interlayer build resolution (i.e., adaptive layer heights).

In this study, we outlined the conceptual foundation for the proposed method and then provided experimental evidence via the results of representative test cases conducted on the developed manufacturing platform. In fact, planning and controlling the nozzle's rotation is a complex task, but we provided a straightforward strategy for its motion. The findings are wrapped up with some critical remarks as follows:

- The proposed method has promising potential for tailoring the interlayer and intralayer build resolutions to fulfill specific needs in future applications. It accomplishes this by employing a change in its effective dimensions to perform the FFF in the same way as if it were carried out with multiple nozzles.
- The potential of the suggested method is explored via four different test cases: The first case experimentally supports the VBW concept, while the second checks its robustness in a difficult task. The third case visualizes a simple wall build with changing resolutions, and the fourth shows how the proposed technique outperforms FFF.
- The first test case shows that discrete effective dimensions of the proposed nozzle and synchronized extrusion rates defined by the related equations yield acceptable results during extrusion on simple tool paths. However, little fine-tuning is necessary to achieve precise dimensions while maintaining the performance.
- The outcomes of the second test demonstrate that the proposed method could be used to make thicker and thinner lines on the same layer. But, a complex motion is yielded by actively guiding the nozzle's alignment. So, dimensional problems are almost certain to arise at the sharp turns. Except for regions of considerable curvature, remarkable precision in achieving the targeted BWs is obtained.
- The maximum achievable layer height increases with the nozzle size in FFF. Hence, a nozzle with a changeable effective dimension allows for flexible layer heights during manufacturing. The third test case visualizes the controlled build resolution in separate local regions of a simple wall.
- With challenging design specifications in its local regions, a vase-like object is manufactured using the proposed method in the fourth test case. This is remarkable since a single nozzle did the production, as the standard FFF approach may require three different-sized nozzles to execute the same task. A conventional 3D printer fails to produce the benchmark object in different scenarios, while the proposed approach produces the vase (the red one) faster and with ease.

It is also important to emphasize that hardware limitations such as the accuracy of the motion axes (i.e., possible inaccuracy when locating the center of the oblong orifice to the axis of rotation) and the controllability of the flow (i.e., a direct-drive extrusion mechanism will be a better choice) can impact the quality of the end products. The continuity equation is used to control the printed trace geometry. But, buckling and twisting of the filament inside the Bowden tube throughout the fabrication process create a considerable transport delay (and backlash) that causes minor variations. Therefore, addressing the following limitations could improve the overall production quality in future studies:

- The extruder-head should rotate within wide range (multiple turns) at high speeds;
- The center of the nozzle's orifice should exactly coincide with the axis of rotation;
- High-torque filament feeding motors should be located very close to the nozzle. The filament is fed to the extruder via a Teflon tube with a length of 70 cm in the current configuration. This arrangement in turn introduces a significant hysteresis nonlinearity in the control loop that makes fine regulation of material flow a challenging task.

Overall, this research provides valuable insights into the use of a controlled-alignment rectangular-orifice nozzle in FFF and demonstrates its potential for adaptable build res-

olution. Although it could have implications for the cost of the specialized equipment, scalability and its integration into existing FFF machines may be further explored to fully realize this potential. Possible future research directions include investigating how the proposed approach might be applied to other forms of additive manufacturing processes.

Another possible field of future research is the development of new process planning methodologies to improve the performance of the rectangular-orifice nozzle, especially at the discontinuity points for convex and concave curves and sharp corners. With further advancements, the presented method may open up new possibilities in terms of design freedom, which could lead to the creation of new products and applications.

Acknowledgements This work was supported in part by the Scientific and Technological Research Council of Turkey (TUBITAK) under the Project Contract 117M429 and Middle East Technical University under the Project Contract ADEP-302-2022-11183.

Funding Open access funding provided by the Scientific and Technological Research Council of Türkiye (TÜBİTAK).

Open Access This article is licensed under a Creative Commons Attribution 4.0 International License, which permits use, sharing, adaptation, distribution and reproduction in any medium or format, as long as you give appropriate credit to the original author(s) and the source, provide a link to the Creative Commons licence, and indicate if changes were made. The images or other third party material in this article are included in the article's Creative Commons licence, unless indicated otherwise in a credit line to the material. If material is not included in the article's Creative Commons licence and your intended use is not permitted by statutory regulation or exceeds the permitted use, you will need to obtain permission directly from the copyright holder. To view a copy of this licence, visit http://creativecommons.org/licenses/by/4.0/.

Appendix A: Process parameters

In this section, a complete list of variables/parameters for designing a rectangular-orifice nozzle is provided, see Table 6.

Appendix B: Filament feeding system

The primary factor contributing to the fluctuation in BW is the inability to effectively control the filament feed-rate on the existing hybrid printing platform. This limitation arises from the utilization of a commercially available extruder head, originally designed for the Ultimaker 3 printer, which has been directly integrated into our system. The positioning of the filament feeder motors in relation to the extruder head was limited by specific design constraints, such as the rotation of the Q-axis. As a result, it was not feasible to place these motors in close proximity to the extruder head. Therefore, it is necessary to introduce the filament, which is propelled by these motors, into the heater located within a lengthy Teflon tube measuring approximately 0.7 m. Figure 15 presents a

Table 6 Independent process parameters (factors) associated with the fabrication process

	Item	Explanation
Input parameters		
1	Rectangular orifice geometry	d_1, d_2
2	Inner geometry of the nozzle	d_0 (the inlet diameter), d_n (the base diameter), l (length of the conical section or cone angle, α)
3	Land of the nozzle	d_L
4	Extruder flow parameters	v (feed-rate), e (extrusion rate)
5	Layer height	h
6	Filament heater / cooling fan	T (effective temperature of the extruded material)
7	Ambient temperature	T_0
8	Extruder head	θ(angular position), $\delta\theta$ (angular positioning error), δe (nozzle eccentricity), δp (positioning error of the linear stages)
9	Extruded material	Polymer type (e.g. PLA, ABS, TPU, PE, PP, etc.) that governs T_c (crystallization temperature of the polymer), ρ (density), ν(T) (viscosity)
10	Nozzle material	Type (e.g. brass, copper, aluminum, stainless steel, etc.) that governs k (heat transfer coefficient), μ (effective kinetic friction coefficient along the inner boundaries of the nozzle) and more
Output parameter		
1	Trace geometry	w (trace width), r (bulging radius of the trace); δh (deviation in the thickness)

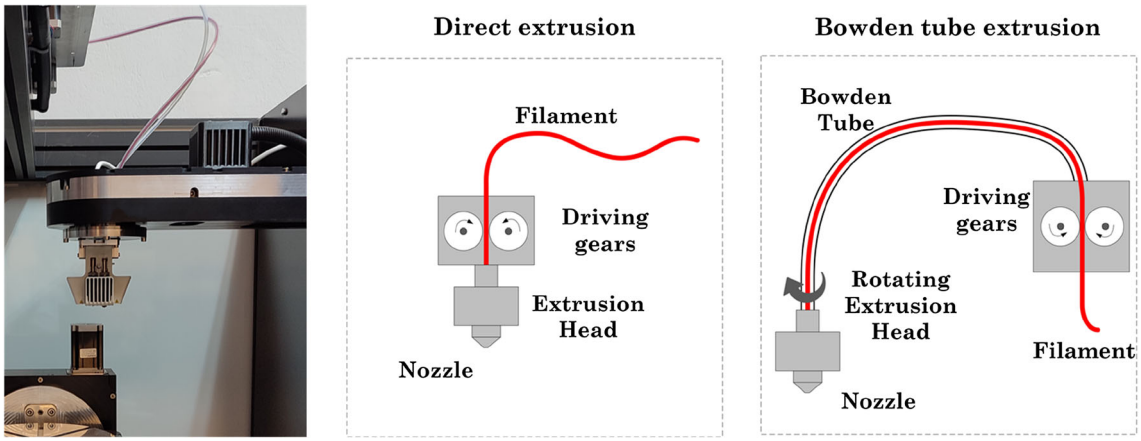

Fig. 15 A detailed photo and a simple schematic showing the Bowden tube extrusion system

comprehensive photograph and a concise schematic depicting the Bowden tube extrusion system.

The research findings indicate that the buckling and twisting of the filament within the tube during the fabrication process result in a significant delay in transportation and backlash in the modulation of the extrusion rate (Moetazedian et al., 2021). Hence, it can be inferred that the observed fluctuations in the feed-rate of the filament are the primary cause of the reported variations.

References

Additive manufacturing—General principles—Terminology (Standard). (2015). International organization for standardization.

Brooks, H., Rennie, A., Abram, T., McGovern, J., & Caron, F. (2011). Variable fused deposition modelling: Analysis of benefits, concept design and tool path generation. In *Proceedings of the 5th international conference on advanced research in virtual and rapid prototyping, Leiria, Portugal* (pp. 511–517).

Chesser, P., Post, B., Roschli, A., Carnal, C., Lind, R., Borish, M., & Love, L. (2019). Extrusion control for high quality printing on big area additive manufacturing (BAAM) systems. *Additive Manufacturing, 28*, 445–455. https://doi.org/10.1016/j.addma.2019.05.020

Di Nisio, F. G., Ventura, H. T., Minetto, R., Dutra, R., & Volpato, N. (2022). A variable bead width filling pattern to print porous media with material extrusion additive manufacturing. *The International Journal of Advanced Manufacturing Technology, 121*(5), 3919–3933. https://doi.org/10.1007/s00170-022-09594-2

Dilberoglu, U. M., Gharehpapagh, B., Yaman, U., & Dolen, M. (2017). The role of additive manufacturing in the era of industry 4.0. *Procedia Manufacturing, 11*, 545–554. https://doi.org/10.1016/j.promfg.2017.07.148

Gharehpapagh, B., Dolen, M., & Yaman, U. (2019). Investigation of variable bead widths in FFF process. *Procedia Manufacturing, 38*, 52–59. https://doi.org/10.1016/j.promfg.2020.01.007

Kuipers, T., Doubrovski, E. L., Wu, J., & Wang, C. C. (2020). A framework for adaptive width control of dense contour-parallel toolpaths in fused deposition modeling. *Computer-Aided Design, 128*, 102907. https://doi.org/10.1016/j.cad.2020.102907

LaBossiere, J. E., Dunn, B. N., Mcdonough, T. J., & Eshelman, M. E. (2009, October). Single-motor extrusion head having multiple extrusion lines [US Patent 7,604,470]. https://patents.google.com/patent/US7604470B2/en

Lind, R. F., Post, B. K., Love, L. J., Lloyd, P. D., Carnal, C. L., Blue, C. A., & Kunc, V. (2017, November). Variable width deposition for additive manufacturing with orientable nozzle [US Patent App. 15/144,957]. https://patents.google.com/patent/US20170320267A1/en.

Löffler, R., & Koch, M. (2019). Innovative extruder concept for fast and efficient additive manufacturing. *IFAC-PapersOnLine, 52*(10), 242–247. https://doi.org/10.1016/j.ifacol.2019.10.071

Moetazedian, A., Budisuharto, A. S., Silberschmidt, V. V., & Gleadall, A. (2021). Convex (continuously varied extrusion): A new scale of design for additive manufacturing. *Additive Manufacturing, 37*, 101576. https://doi.org/10.1016/j.addma.2020.101576

Myerberg, J. S., Fulop, R., Gibson, M. A., Hart, J. A., Fontana, R. R., Schuh, A. C., Chiang, Y.-M., Verminski, D. M., Schmitt, A. P., Sachs, M. E., & Chin, R. (2018). Fused filament fabrication nozzle with controllable exit shape [US Patent 0,311,738]. https://patents.google.com/patent/US20180311738A1/en.

Tan, L. J., Zhu, W., & Zhou, K. (2020). Recent progress on polymer materials for additive manufacturing. *Advanced Functional Materials, 30*(43), 2003062. https://doi.org/10.1002/adfm.202003062

Vanacker, G. (2017, January). 3D printing system and process [EP3117982A1]. https://patents.google.com/patent/EP3117982A1/en.

Wang, J., Chen, T.-W., Jin, Y.-A., & He, Y. (2019). Variable bead width of material extrusion-based additive manufacturing. *Journal of Zhejiang UniversitySCIENCE A, 20*(1), 73–82.

Wu, P., Ramani, K. S., & Okwudire, C. E. (2021). Accurate linear and nonlinear model-based feedforward deposition control for material extrusion additive manufacturing. *Additive Manufacturing, 48*, 102389. https://doi.org/10.1016/j.addma.2021.102389

Xu, J., Ding, L., Cai, L., Zhang, L., Luo, H., & Qin, W. (2019). Volume-forming 3D concrete printing using a variable-size square nozzle. *Automation in Construction, 104*, 95–106. https://doi.org/10.1016/j.autcon.2019.03.008

Publisher's Note Springer Nature remains neutral with regard to jurisdictional claims in published maps and institutional affiliations.